AER/AGS Open File Report 2021-05

Alberta Energy Regulator

Temperature Mapping of Select Devonian Strata in Alberta

AGS
ALBERTA GEOLOGICAL SURVEY

AER/AGS Open File Report 2021-05

Temperature Mapping of Select Devonian Strata in Alberta

J. Brinsky, A. Singh, T.E. Hauck, M. Grobe and D. Palombi

Alberta Energy Regulator
Alberta Geological Survey

June 2022

ISBN 978-1-4601-5353-6

Brinsky, J, Singh, A., Hauck, T.E., Grobe, M. and Palombi, D. (2022): Temperature mapping of select Devonian strata in Alberta; Alberta Energy Regulator / Alberta Geological Survey, AER/AGS Open File Report 2021-05, 28 p.

Published June 2022 by:
Alberta Energy Regulator
Alberta Geological Survey
4th Floor, Twin Atria Building
4999 – 98th Avenue
Edmonton, AB T6B 2X3
Canada

Tel: 780.638.4491
Email: AGS-Info@aer.ca
Website: www.ags.aer.ca

Contents

Acknowledgements vi
Abstract vii
1 Introduction 1
2 Background 1
2.1 Previous Temperature Mapping 1
2.2 Sources of Temperature Data and Correction Methods 1
2.3 Geology of the Alberta Basin 2
3 Data and Methodology 5
3.1 Initial Culling Steps 6
3.2 Bottomhole Temperature Correction 7
3.3 Statistical Culling 10
3.4 Three-Dimensional Model and Mapping 10
4 Results 11
5 Limitations 12
6 Summary 16
7 References 17
Appendix 1 – Temperature Maps 19

Tables

Table 1. Number of data points in the two datasets before and after statistical culling. Nieuwenhuis dataset contains data from Nieuwenhuis et al. (2015) study. 10
Table 2. Model input parameters used to create the three-dimensional subsurface temperature model. 11
Table 3. Temperature distribution summary for formation/group-scale maps created from the updated temperature model. 16

Figures

Figure 1. Depth to the Precambrian basement as contours (500 m interval) on a digital elevation model of the land surface. 3
Figure 2. Structural cross-section A–A' running along strike of the Alberta Basin. 4
Figure 3. Structural cross-section B–B' running along the dip of the Alberta Basin. 5
Figure 4. Temperature versus depth plots of the raw bottomhole temperature data. 6
Figure 5. Temperature versus depth plot of the raw bottomhole temperature data. 7
Figure 6. Example of the Harrison-correction equation process from Twp. 11, Rge. 27, W 4th Mer., Alberta. 8
Figure 7. Combined plot of the temperature data used to create a new correction equation for Alberta subsurface temperature data. 9
Figure 8. Best-fit plot of bottomhole temperature data corrected using the second-order polynomial equation, and co-located temperatures from the Nieuwenhuis et al. dataset. 9
Figure 9. Comparison of the original Harrison equation with the Harrison equation based on calibration with Alberta data. 12
Figure 10. Locations of recorded temperatures, included in the Nieuwenhuis et al. dataset. 13
Figure 11. Locations of recorded temperatures, included in the Alberta-calibrated Harrison-corrected bottomhole temperature dataset. 14
Figure 12. Increase in data points per township resulting from the addition of the bottomhole temperature dataset to the Nieuwenhuis et al. dataset. 15
Figure 13. Temperature at the base of the Wabamun Group. 20
Figure 14. Temperature at the base of the Winterburn Group. 21

Figure 15. Temperature at the base of the Leduc Formation. 22
Figure 16. Temperature at the base of the contiguous Swan Hills and Slave Point formations. 23
Figure 17. Temperature at the base of the Watt Mountain Formation. 24
Figure 18. Temperature at the base of the Sulphur Point Formation. 25
Figure 19. Temperature at the base of the Keg River Formation 26
Figure 20. Temperature at the top of the Precambrian 27
Figure 21. Thermal gradient calculated at the top of the Precambrian. 28

Acknowledgements

We thank Eric Timmer (Alberta Geological Survey) for his help with data compilation and processing. We thank Jacek Majorowicz and his colleagues for allowing the temperature data produced at the University of Alberta during the Helmholtz-Alberta Initiative and his prior research to be included in our data compilation for this study.

Abstract

This report presents the results and findings of a subsurface temperature mapping project conducted by the Alberta Geological Survey. Alberta's long history of petroleum exploration has resulted in a wealth of temperature data, from various sources and of varied quality. Temperature measurements from drillstem tests and annual pool pressure surveys are considered higher quality, whereas temperature measurements recorded from wireline logs as bottomhole temperatures (BHT) are considered lower quality. The BHTs often reflect the temperature of drilling mud in the wellbore, which has not equilibrated with the formation temperature, and the temperatures need to be corrected to be representative of in situ conditions. To maximize the amount of BHT data available for this project, a temperature correction method based on a derivation of the Harrison correction was developed. The resulting Alberta-calibrated Harrison equation was applied to previously unused BHT data to estimate more accurate formation temperatures. These corrected BHTs were then merged with a pre-existing temperature dataset to provide an updated subsurface temperature database for the Alberta Basin. A three-dimensional subsurface temperature model was generated using the new database. Two-dimensional temperature maps were produced for some of Alberta's deeper sedimentary formations that may be targeted for future geothermal exploration and development. Units mapped for this project are, in descending stratigraphic order, the Wabamun Group, the Winterburn Group, the Leduc Formation, the contiguous Swan Hills and Slave Point formations, the Watt Mountain Formation, the Sulphur Point Formation, and the Keg River Formation. In addition, the temperature at the top of the Precambrian crystalline basement (base of the sedimentary succession) was also mapped. An updated thermal gradient map of the Alberta Basin was produced, which provides an estimate of the average temperature increase with depth from the surface to the top of the Precambrian.

1 Introduction

Alberta's long history of petroleum exploration and development has resulted in a vast array of subsurface temperature measurements in the Alberta Basin. Subsurface temperature is measured during various operations in oil and gas wells, including wireline logging, drillstem testing, and well pressure testing. These temperature data are recorded on wireline logs as bottomhole temperatures (BHTs), or in drillstem test (DST) and well pressure survey (performed during annual pool pressure survey) reports, but the data are of various quality. Understanding subsurface temperature is necessary for geothermal resource characterization and is also important for other resource evaluations including hydrocarbon maturation and minerals precipitation. The demand for subsurface temperature data and map products has increased recently, with Albertans, industry, and governments actively considering geothermal energy as a renewable energy option in Alberta. Geothermal energy is being used for residential heating and cooling and is showing potential for commercial applications and possibly for providing baseload electricity generation.

This project focused on making existing BHT data usable by applying corrections to erroneous data. This new dataset was merged with a pre-existing temperature dataset to produce an updated distribution of subsurface temperature in Alberta as a three-dimensional (3D) empirical Bayesian kriging model. This new model used the Alberta Geological Survey's (AGS) Geological Framework of Alberta (Alberta Geological Survey, 2021) to render two-dimensional (2D) formation/group-scale temperature maps for some of Alberta's deeper sedimentary formations, which may be targeted for future geothermal exploration and development. It also enabled the creation of an updated thermal gradient map, calculated at the base of the sedimentary succession (the top of the Precambrian).

2 Background

2.1 Previous Temperature Mapping

Over the last few decades, various authors mapped the subsurface temperature in Alberta. Early work by the American Association of Petroleum Geologists included a temperature database and geothermal gradient map of North America (Geothermal Survey of North America; Kehle et al., 1970; DeFord and Kehle, 1976). Jones et al. (1985) created temperature maps for the Paleozoic and Precambrian surfaces in Alberta from 55 246 BHT measurements. Bachu and Burwash (1994) mapped the integral geothermal gradient at the top of the Precambrian throughout the Western Canada Sedimentary Basin (WCSB). Weides and Majorowicz (2014) mapped the geothermal gradient and heat flow for the WCSB and created temperature maps for several formations in the WCSB. A 3D subsurface temperature model was created by Nieuwenhuis et al. (2015) and used to publish 2D maps for various depths across the basin. Numerous other geothermal studies included mapping and evaluating formation temperature in Alberta at the subregional scale (e.g., Lam and Jones, 1985, 1986; Gray et al., 2012; Majorowicz et al., 2012; Weides et al., 2013, 2014; Banks and Harris, 2018).

2.2 Sources of Temperature Data and Correction Methods

The main sources of subsurface temperature data in Alberta are DSTs, well pressure surveys, and wireline logging (BHTs), all obtained during oil and gas exploration and production activities. Lengyel (2013) analyzed and described the apparent errors in temperature data from these sources and applied standardized quality coding to the data.

Drillstem tests are performed during or shortly after drilling a well by isolating a selected interval and allowing formation flow and pressure buildup periods. During this test, downhole thermometers record the temperature of the wellbore fluids. Drillstem tests that recover formation fluids are generally regarded as a reliable source of temperature data. Conversely, DSTs in wells that contain drilling fluids, such as mud and fluid cushion to help maintain pressure balances in the wellbore, along with DSTs that recover

small amounts of or no formation fluids are considered less reliable. In addition, DSTs that are performed in mature hydrocarbon pools may have temperatures influenced by nearby water flood activities (Gray et al., 2012).

Well pressure surveys are routinely performed in Alberta as part of the Alberta Energy Regulator's Directive 040 requirements (Alberta Energy Regulator, 2021). The pressure surveys often include recording the subsurface temperature and are considered a reliable source of data, provided the well has been shut in for an appropriate amount of time or has not been introduced to load fluids recently.

The BHT recordings provide a vast amount of temperature data in Alberta. Typically, these temperatures are recorded when various wireline tools are run downhole to measure reservoir properties after drilling a well. These logging tools include a thermometer that records the maximum temperature encountered. At the time of recording, drilling mud that has been circulated throughout the wellbore is still present. The presence of the drilling mud results in a recorded temperature of fluid that has not equilibrated to the formation temperature and requires a correction to be representative of the in situ temperature.

Different methods of varying complexity have been derived and used to correct BHTs to reservoir temperature. Two common correction methods used in Alberta are the Horner correction (Horner, 1951) and the Harrison correction (Harrison et al., 1983). The Horner correction was initially developed for pressure equilibration to predict reservoir formation pressure. A similar method is used to correct temperatures. To perform a Horner correction, multiple temperature recordings taken at different times are required. Additional data requirements include the amount of time the well was circulated during drilling, and the amount of time between the end of mud circulation and when the temperature measurement was recorded. These additional data are not always available or easily accessible, which limits the number of temperature measurements that can be efficiently corrected using the Horner method.

The Harrison correction (Harrison et al., 1983) is a second-order polynomial equation developed by the Oklahoma Geological Survey by calibrating BHTs with high quality temperature data from DSTs and well pressure surveys in the Oklahoma Basin. As this correction can be performed with only the depth and temperature reported, it was more suited to the data in this study.

Maximum temperature thermometers, used in DSTs, BHTs, and well pressure surveys, present problems when recording formation temperatures in the shallow subsurface (<1000 m deep), where the temperature can be cooler than ambient air at the surface, particularly during the summer months (Gray et al., 2012; Majorowicz et al., 2012; Lengyel, 2013). As a result, shallow subsurface temperature data are often biased towards higher temperatures, especially those data collected prior to the mid-1990s when maximum temperature thermometers were replaced by digital thermometers as the industry standard (Gray et al., 2012). To avoid this issue, this project was limited to data from depths greater than 1000 m.

2.3 Geology of the Alberta Basin

The Alberta Basin (Figure 1)—part of the WCSB—is a northwest-trending trough parallel to the Rocky Mountain fold-and-thrust belt (Wright et al., 1994). The Phanerozoic sedimentary succession rests unconformably on the Precambrian basement and comprises a wedge-shaped package of rocks that thins progressively eastwards towards the Canadian Shield in northeastern Alberta (Figures 2 and 3). The basin fill comprises two broad sedimentary bedrock packages: (1) a lower Paleozoic to Middle Jurassic interval, dominated by carbonate rocks, evaporites, and terrigenous shales, recording deposition in shallow seas along the western margin of Laurentia; and (2) an Upper Jurassic to lower Cenozoic succession of siliciclastic rocks, which were deposited in front of the evolving Canadian Cordillera. Bedrock is overlain by a Paleogene to Quaternary sediment cover of variable thickness (Figures 2 and 3). The undeformed sediments package approaches 5 km in thickness in the deepest part of the basin in front of the Cordillera.

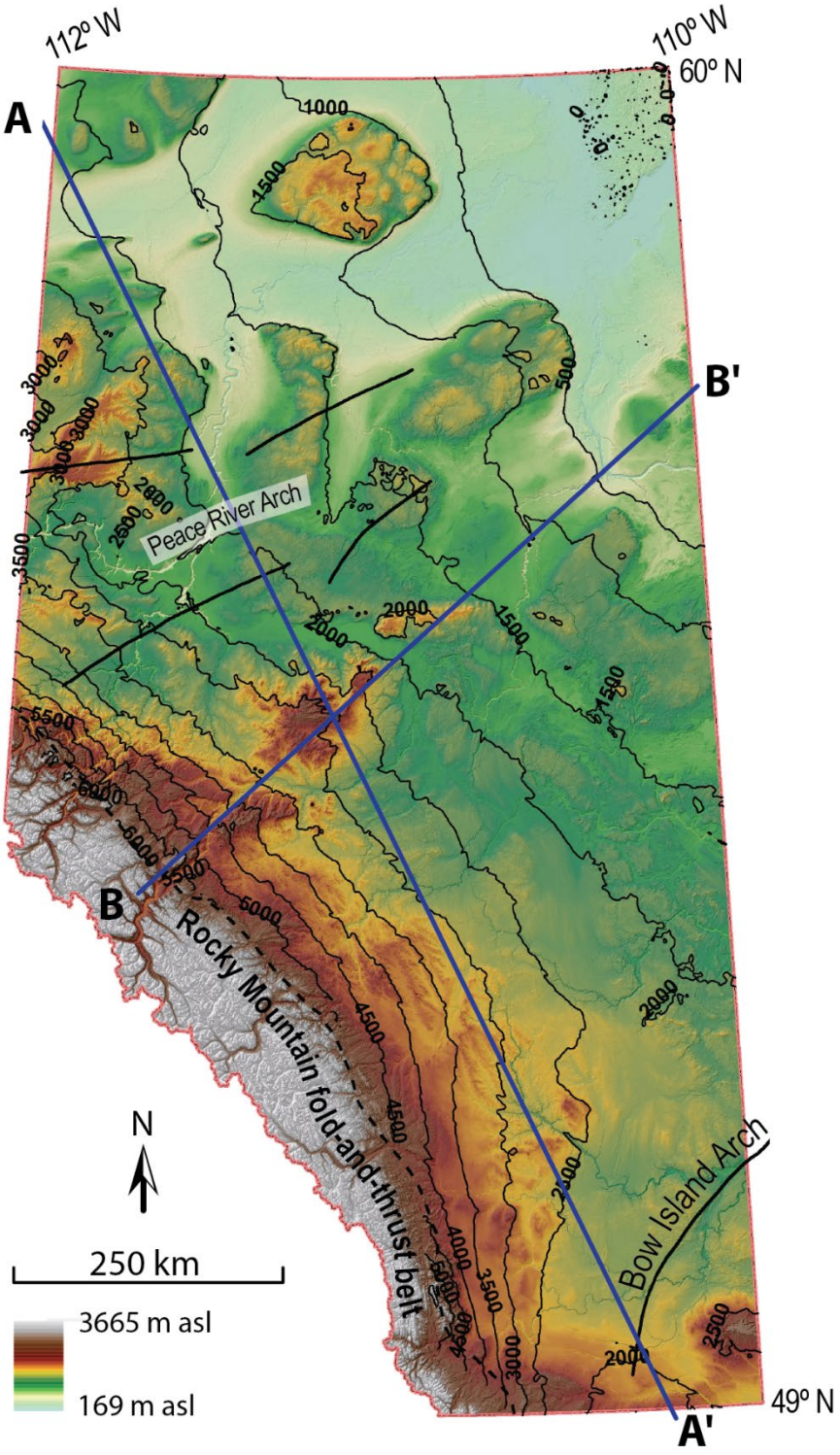

Figure 1. Depth to the Precambrian basement as contours (500 m interval) on a digital elevation model (U.S. Geological Survey, 2014) of the land surface. Two major structural basement elements are shown: the Peace River Arch (O'Connell, 1994) and the Bow Island Arch (Kent and Christopher, 1994). Lines of cross-sections in Figures 2 and 3 are shown.

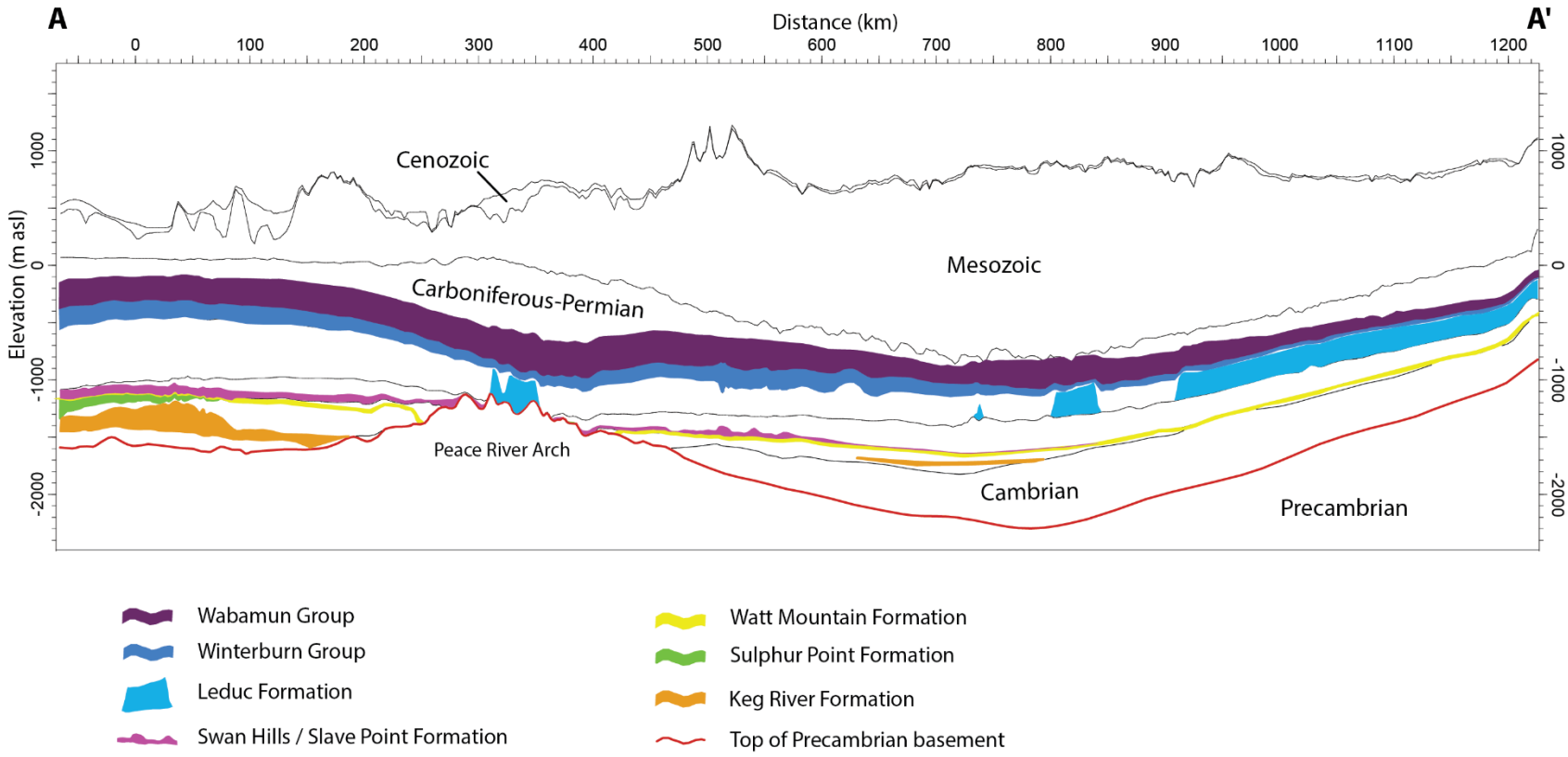

Figure 2. Structural cross-section A–A' running along strike of the Alberta Basin (see Figure 1 for location). Temperature maps were created for the bases of the geological units indicated and for the top of the Precambrian crystalline basement. Vertically exaggerated 100 times.

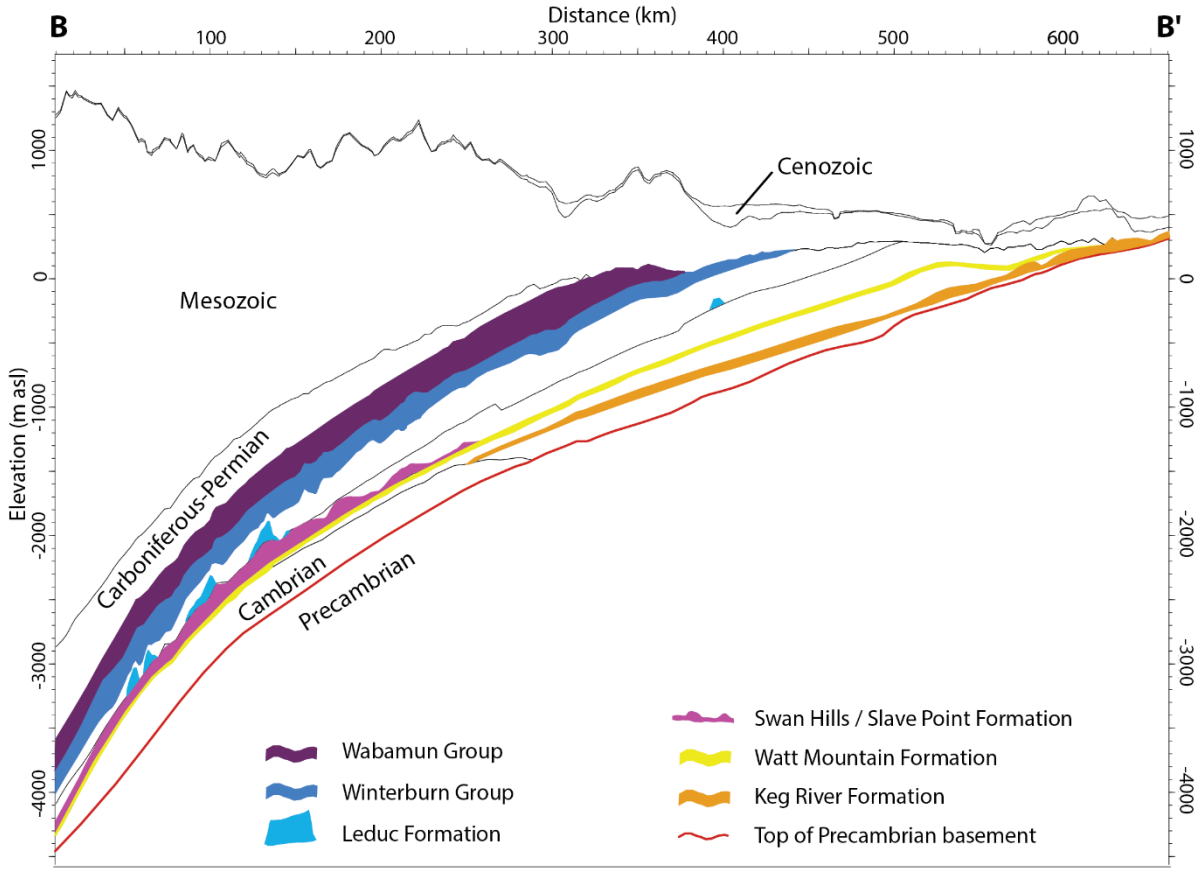

Figure 3. Structural cross-section B–B' running along the dip of the Alberta Basin (see Figure 1 for location). Temperature maps were created for the bases of the geological units indicated and for the top of the Precambrian crystalline basement. Vertically exaggerated 75 times.

The deep Devonian units in the western part of the province (Figures 2 and 3) are the preferred targets for geothermal exploration due to their known (or expected) favourable rock properties, as well as higher temperatures. Units mapped in this report are, in descending stratigraphic order: (1) the Wabamun Group, (2) the Winterburn Group, (3) the Leduc Formation, (4) the contiguous Swan Hills and Slave Point formations, (5) the Watt Mountain Formation, (6) the Sulphur Point Formation, and (7) the Keg River Formation. In addition, the temperature at the top of the Precambrian crystalline basement (base of the sedimentary succession) was also mapped.

With the exception of the Watt Mountain Formation, the Devonian units all comprise variably dolomitized carbonate strata. Some of the carbonate rocks, such as in the Leduc, Swan Hills, and Slave Point formations, are buildups of limited extent, whereas others are broad tabular units with basin-wide extent (Figures 2 and 3). The Sulphur Point Formation is a wedge-shaped Middle Devonian unit of the Elk Point Group that is limited to the northwestern part of the province (Figure 2). The Watt Mountain Formation—the uppermost unit of the Elk Point Group—is a shaly unit that includes sandstone of the Gilwood Member. The Gilwood Member is restricted to the flanks of the Peace River Arch (Figure 2).

3 Data and Methodology

Three different sources of temperature data were used in this project: DSTs, well pressure surveys, and wireline logs (BHTs). Bottomhole temperatures were extracted from well log data files in Log ASCII Standard (LAS) format (Alberta Energy Regulator, 2022) and were added to an existing legacy database

of BHTs, created at the AGS in the 1990s and early 2000s by manually transcribing log header data from microfiche logs. When the depth of a temperature measurement was not reported for a BHT, the total depth of the well (in true vertical depth) was used as an approximation. The assembled BHT dataset contained raw temperatures recorded in both Celsius and Fahrenheit. A culling procedure was required to remove erroneous outliers prior to use.

An additional temperature dataset was obtained from the University of Alberta through a data sharing agreement. The Nieuwenhuis et al. (2015) study produced this dataset (referred to as the 'Nieuwenhuis dataset' in this report) under the Helmholtz-Alberta Initiative and prior research by Dr. Jacek Majorowicz. Temperatures were obtained from DSTs, well pressure surveys, and wireline logs (Horner-corrected BHTs). Depths from this dataset were corrected from measured depth to true vertical depth, where required.

3.1 Initial Culling Steps

Initial analysis of the BHT dataset revealed a high frequency of data points with recorded BHTs of exactly 100°C and 100°F for various depths (Figure 4). Lengyel (2013) also noticed the anomalously high frequency of 100°F measurements in DSTs and reported that these temperatures were often estimated before the test, and were not representative of the actual BHT. The high frequency of the 100°C and 100°F in this BHT dataset raised suspicions that some of these temperatures had also been estimated. As a precaution, all temperature measurements of exactly 100°C or 100°F were deemed unreliable and were removed from the BHT dataset. Similarly, the numerous data points with a reported temperature of 0°C were also removed.

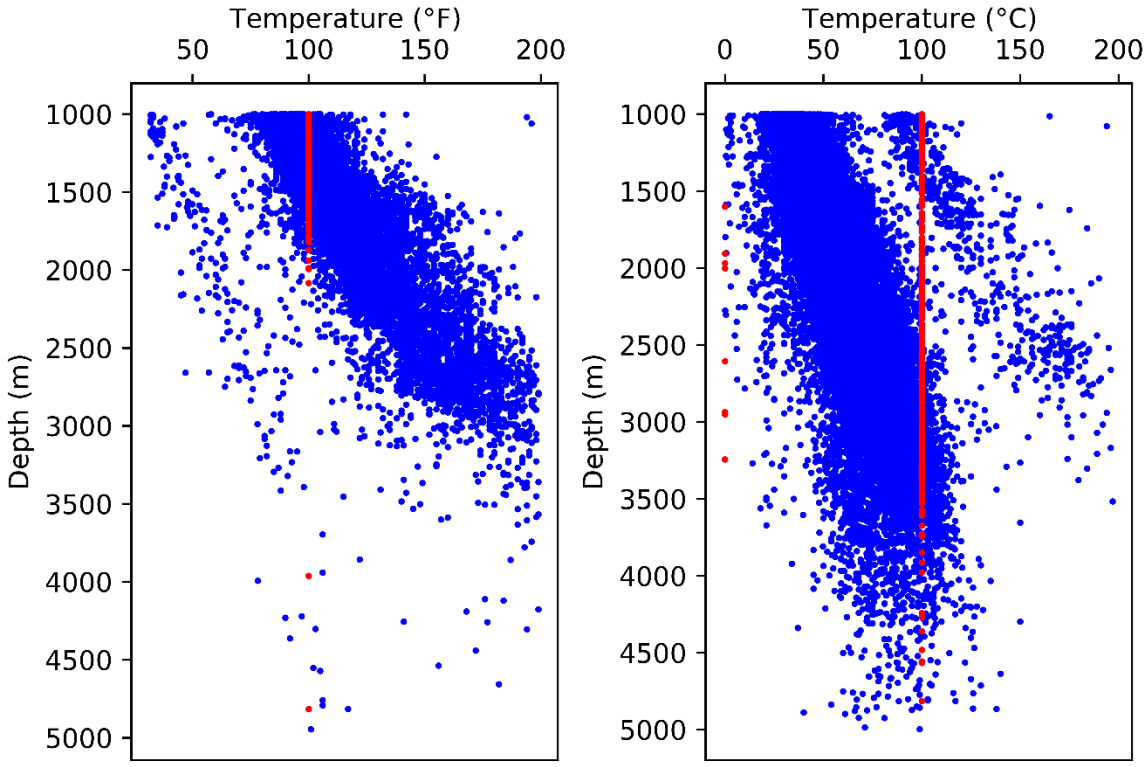

Figure 4. Temperature versus depth plots of the raw bottomhole temperature data. Temperature measurements of 100°C, 100°F, and 0°C (red dots) were deemed unreliable and were removed from the dataset. Depths were measured from the kelly bushing height on the drilling rig floor.

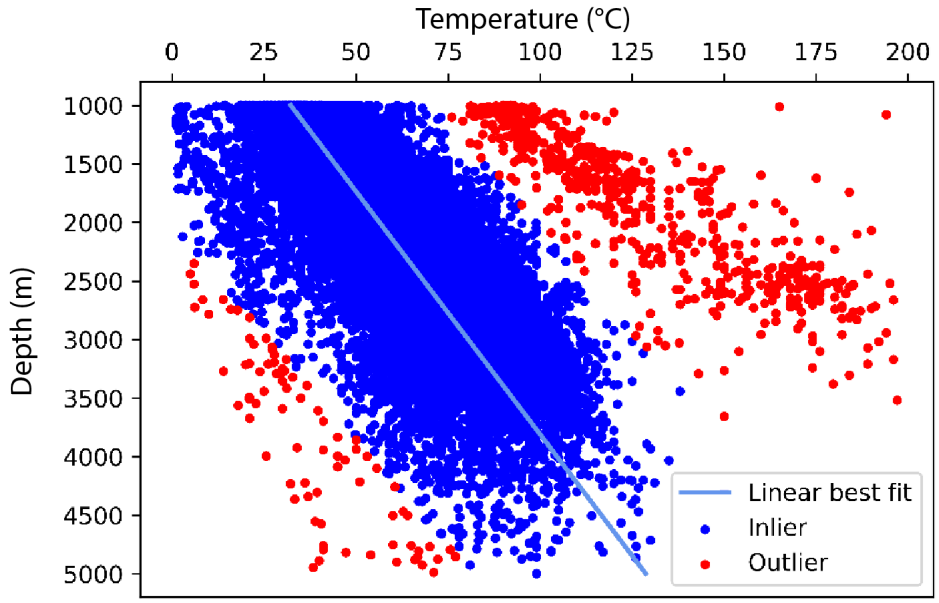

Figure 5. Temperature versus depth plot of the raw bottomhole temperature data. Data points in red are greater than 2.5 standard deviations from the main trend and were considered outliers and removed from the final dataset. Depths were measured from the kelly bushing height on the drilling rig floor.

Further analysis of the BHT dataset revealed a predominant temperature versus depth trend with two additional trends at both hotter and cooler temperatures. Spatially, these hotter and cooler temperature data appeared anomalous compared to surrounding temperature measurements. Further investigation into these data showed the anomalous trends on the temperature versus depth plot were often the result of unit conversion or data entry error, that is, the temperature was measured in Celsius but recorded in Fahrenheit or vice versa. To deal with these anomalous trends in an efficient manner, a trend line was fit to the data and data points greater than 2.5 standard deviations above and below this trend line were considered outliers and removed from the final dataset (Figure 5).

3.2 Bottomhole Temperature Correction

To maximize the amount of BHT data available to use in this project, a temperature correction method based on a derivation of the Harrison equation was used. The approach used the Nieuwenhuis dataset as training data to calibrate the BHTs. Data from the BHT dataset and the Nieuwenhuis dataset were grouped based on the township and range of the survey site.

For each township that contained at least five data points from the Nieuwenhuis dataset, a geothermal gradient was fit with an x-intercept temperature of 5°C. The 5°C surface temperature approximation is similar to what has been used in other studies, which entailed more complex interpolations of ground surface temperature measurements (Bachu and Burwash, 1994). However, some studies have used an x-intercept temperature of 0°C (e.g., Weides and Majorowicz, 2014; Weides et al., 2014) because of evidence that deeper geothermal gradients may still be in equilibrium with ice-age, subglacial ground surface temperatures (Majorowicz et al., 2012). A sensitivity analysis was performed by changing the x-intercept to 0°C, which revealed the change was not impactful for the depths in this project's dataset (>1000 m). On the gradient plot for the township, BHT data from the same township were plotted. The mean temperature deviation from the geothermal gradient in each township was determined by using the mean BHT recording depth, along with the mean temperature deviation from the geothermal gradient (Figure 6).

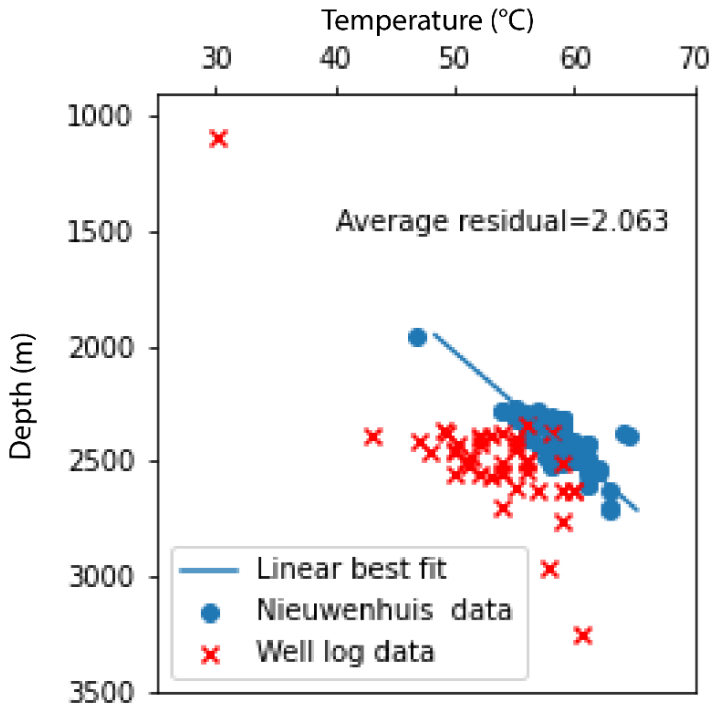

Figure 6. Example of the Harrison-correction equation process from Twp. 11, Rge. 27, W 4th Mer., Alberta. Nieuwenhuis data from Nieuwenhuis et al. (2015) dataset; well log data from this project's bottomhole temperature dataset. Depths were measured from the kelly bushing height on the drilling rig floor.

The average temperature deviation and average depth of the recorded temperatures for each township were then plotted, resulting in data from approximately 2100 townships (Figure 7). Initially, three different trend lines were fit to the data including a second-order polynomial, third-order polynomial, and an exponential fit. The r^2 values of the three fits were similar, with values of 0.95, 0.95, and 0.94. The corresponding equation derived from these fits was then applied to the original temperature recorded during wireline logging resulting in a corrected temperature.

An analysis was then performed by plotting the corrected BHTs to temperatures from DSTs and well pressure surveys (from the Nieuwenhuis dataset) that were co-located in depth to determine the accuracy of each correction method (Figure 8). To avoid overfitting the data, and to maintain consistency with the original Harrison equation, the second-order polynomial equation was ultimately used, giving an Alberta-calibrated Harrison-correction equation of

$$Tc = -13.6586 + 0.01806\,x - 0.000002555\,x^2$$

where Tc = temperature increase to equilibrium; and x = depth in metres.

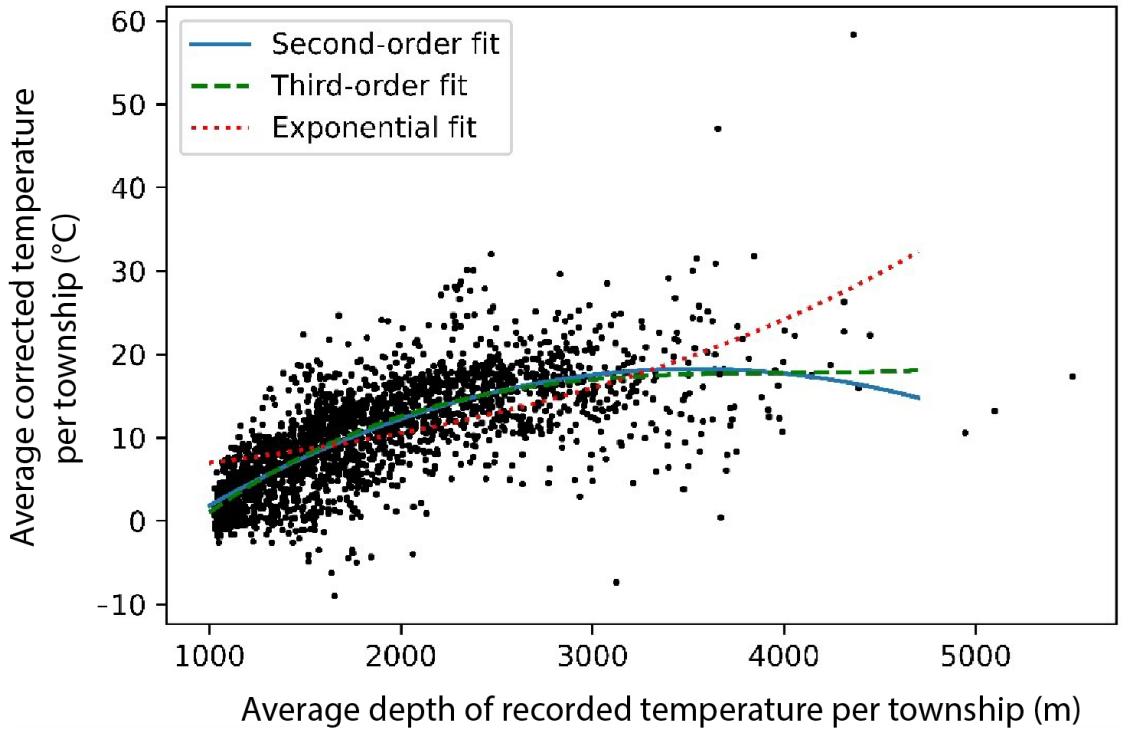

Figure 7. Combined plot of the temperature data used to create a new correction equation for Alberta subsurface temperature data. Depths were measured from the kelly bushing height on the drilling rig floor.

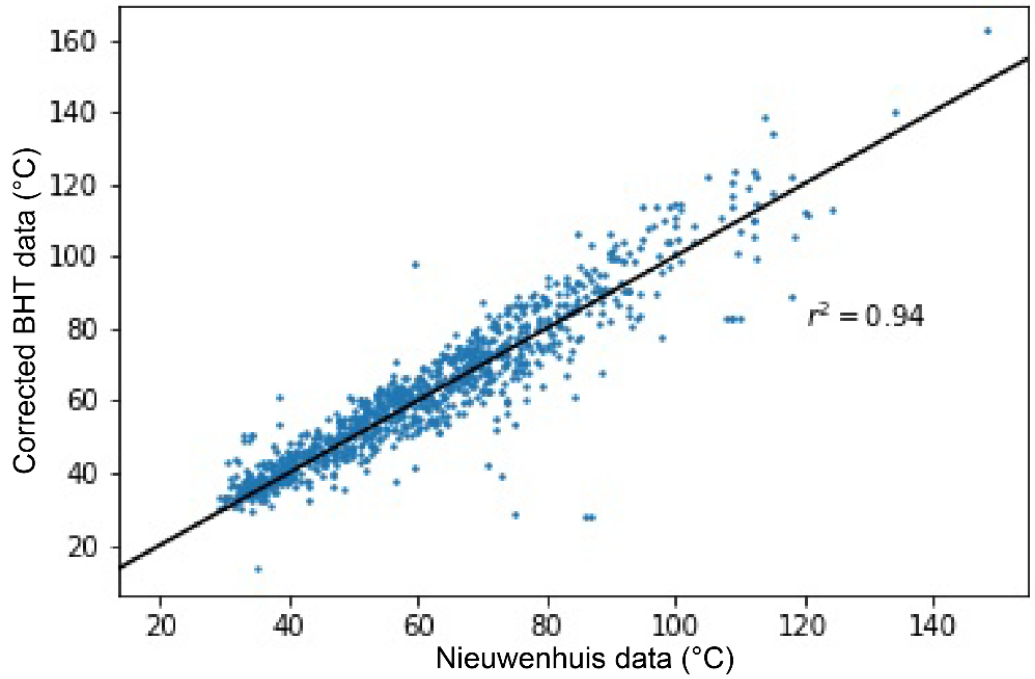

Figure 8. Best-fit plot of bottomhole temperature (BHT) data corrected using the second-order polynomial equation, and co-located temperatures from the Nieuwenhuis et al. (2015) dataset.

3.3 Statistical Culling

The Alberta-calibrated Harrison correction was applied to all temperatures in the BHT dataset to represent the predicted subsurface temperature. A statistical method similar to that used by Nieuwenhuis et al. (2015) was deployed in this project to remove any outliers remaining in the database. Prior to statistical culling, the database consisted of 133 231 data points from the BHT dataset and 126 108 from the Nieuwenhuis dataset. The statistical culling method first focused on removing data from the BHT dataset that appeared anomalous compared to surrounding data points, and then removing data points from both datasets that had a large residual (predicted value minus the measured value) when modelled using empirical Bayesian kriging. The approach was as follows:

1) Combine and model the data using 3D empirical Bayesian kriging. Analyze the data using cross-validation and remove BHT data points that have a cross-validation error greater than 2.5 or less than –2.5 standard deviations from the mean error.
2) Remodel the remaining data and remove BHT data points with a cross-validation error greater than 2.5 standard deviations from the mean error.
3) Remodel the remaining data and calculate residuals (predicted value minus measured value). Remove BHT and Nieuwenhuis data points with a residual greater than 5°C or less than –5°C.

The statistical culling removed 27 978 data points from the BHT dataset and 659 from the Nieuwenhuis dataset, leaving a final temperature database of 230 702 data points (Table 1; Brinsky et al., 2022a).

3.4 Three-Dimensional Model and Mapping

The Devonian portion of the Paleozoic sedimentary succession was the focus of this project. In addition, the top of the Precambrian basement was analyzed (Figures 2 and 3). Temperature maps for the Devonian units were produced from temperature predictions proximal to the base of the strata (e.g., base of the Sulphur Point Formation). Therefore, the maps approximate the temperature at the top of the underlying formation as well. For example, the temperature at the base of the Wabamun Group can also be considered the temperature at the top of the underlying Winterburn Group.

The final data were then modelled with depth using the model input parameters shown in Table 2, creating a 3D subsurface temperature model. The resulting model had both a root-mean-square error and average standard error of 1.23°C.

The predictions from the model were exported as point data created at a 500 m x,y sampling interval, at the depth of the base of the formation/group selected to map (discussed in Section 2.3). The depth to the base of the formation/group was calculated by adding the depth to the top of the formation/group grid to a vertical thickness grid. Modelled thickness grids for the mapped formations/groups were derived from version 3 of AGS's Geological Framework of Alberta (Alberta Geological Survey, 2021). The point data were modelled using empirical Bayesian kriging and the final map was clipped to an area where the depth to the top of the formation/group is greater than 1000 m.

Table 1. Number of data points in the two datasets before and after statistical culling. Nieuwenhuis dataset contains data from Nieuwenhuis et al. (2015) study.

Dataset	Pre-Statistical Cull	Post-Statistical Cull
Nieuwenhuis	126 108	125 449
Bottomhole temperature	133 231	105 253
	Final database	230 702

Table 2. Model input parameters used to create the three-dimensional (3D) subsurface temperature model.

Parameter	Description
Method	Empirical Bayesian kriging 3D
Transformation type	Empirical
Semivariogram model type	Exponential
Subset size	100
Overlap factor	1
Number of simulations	100
Elevation inflection factor	63
Trend	First

An updated thermal gradient map was also produced by dividing the temperature at the top of the Precambrian (base of the sedimentary succession) by the depth to the top of the Precambrian.

In addition, a dataset of temperature predictions was exported with x,y spacing of 4000 m, and z values starting at 1000 m with sampling every 125 m down to the top of the Precambrian basement (Brinsky et al., 2022b). In addition to the temperature maps, grid products were exported for selected Devonian strata and are available in ASCII format (Brinsky et al., 2022c). This was then expanded to include several formations and groups spanning from the uppermost Devonian to the Jurassic (Brinsky et al., 2022c): Exshaw Formation, Rundle Group, Montney Formation, Doig Formation, Halfway Formation, and Fernie Formation.

4 Results

When compared to the original Harrison equation, the new Alberta-calibrated Harrison equation applies a larger temperature correction at depths from 1000 to 3250 m and a smaller correction at depths greater than 3250 m (Figure 9). On average the mean correction applied to the BHTs in the final dataset was 8.7°C.

The final Nieuwenhuis dataset consisted of 125 449 temperature measurements: 94 742 from well pressure surveys, 29 430 from DSTs, and 1277 from wireline logs (Horner-corrected BHTs; Figure 10). An additional 105 253 BHT data points were added to the Nieuwenhuis dataset (Figure 11). This addition of the new Alberta-calibrated Harrison-corrected temperature data resulted in a data increase for 4004 townships (Figure 12), with some townships seeing a large increase in data density (e.g., greater than 200 data points per township). Formation/group-scale temperature maps were created for the base of the Wabamun and Winterburn groups, the Leduc, Swan Hills / Slave Point, Watt Mountain, Sulphur Point, and Keg River formations (Appendix 1, Figures 13–19), and for the top of the Precambrian crystalline basement (Appendix 1, Figure 20). A summary of the temperature distribution by areal extent (shown in sections) for the mapped formations/groups is shown in Table 3.

The thermal gradient map shows an estimate of the average temperature increase from the surface to the top of the Precambrian basement. The values range from a low of <25°C/km in the southwestern part of the province to over 50°C/km in the northwest (Appendix 1, Figure 21).

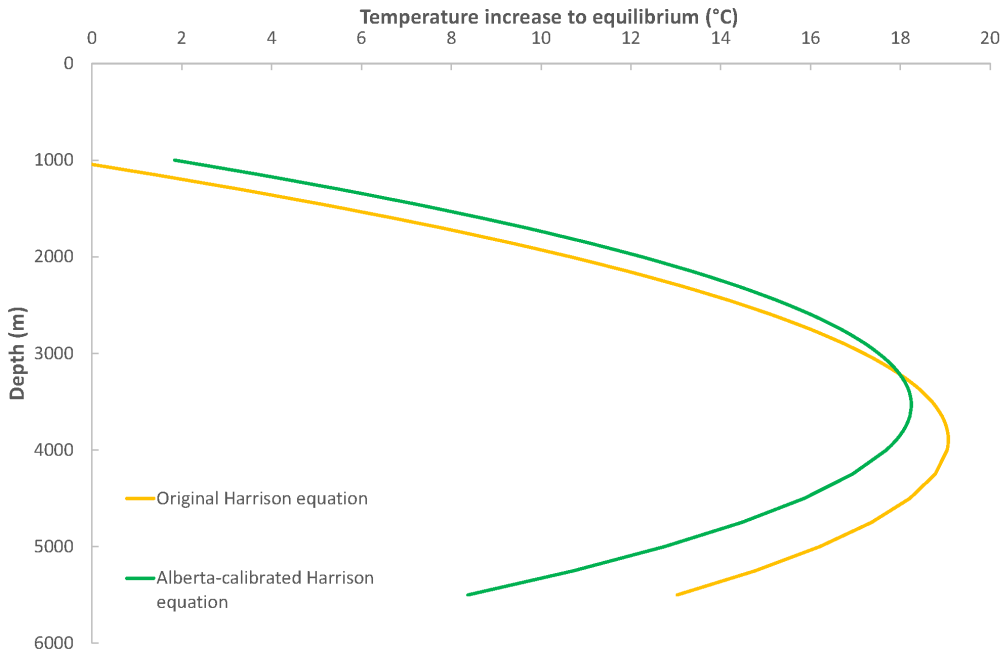

Figure 9. Comparison of the original Harrison equation (Harrison et al., 1983) with the Harrison equation based on calibration with Alberta data. Depths were measured from the kelly bushing height on the drilling rig floor.

5 Limitations

The temperature maps and model produced in this project provide a good regional representation of the subsurface temperature distribution in Alberta, although certain limitations exist. As a result of the statistical culling process, potential local anomalies that varied from surrounding temperatures may have been removed. Temperatures in the shallow subsurface (<1000 m deep) were excluded to deal with false temperature measurements that may occur in the shallow subsurface. As a result, the maps produced only provide temperature predictions for depths where the formation top is >1000 m deep. The thermal gradient map, which uses the temperature and depth of the Precambrian top, assumes a linear gradient from the surface. Although this thermal gradient can be used to estimate the temperature at a given depth, the thermal conductivity of the rocks and pore fluids does vary throughout the sedimentary succession, which results in a variation of the rate of temperature increase.

The results are intended to represent the temperature distribution at the regional scale. For local-scale use, more detailed analyses would be needed.

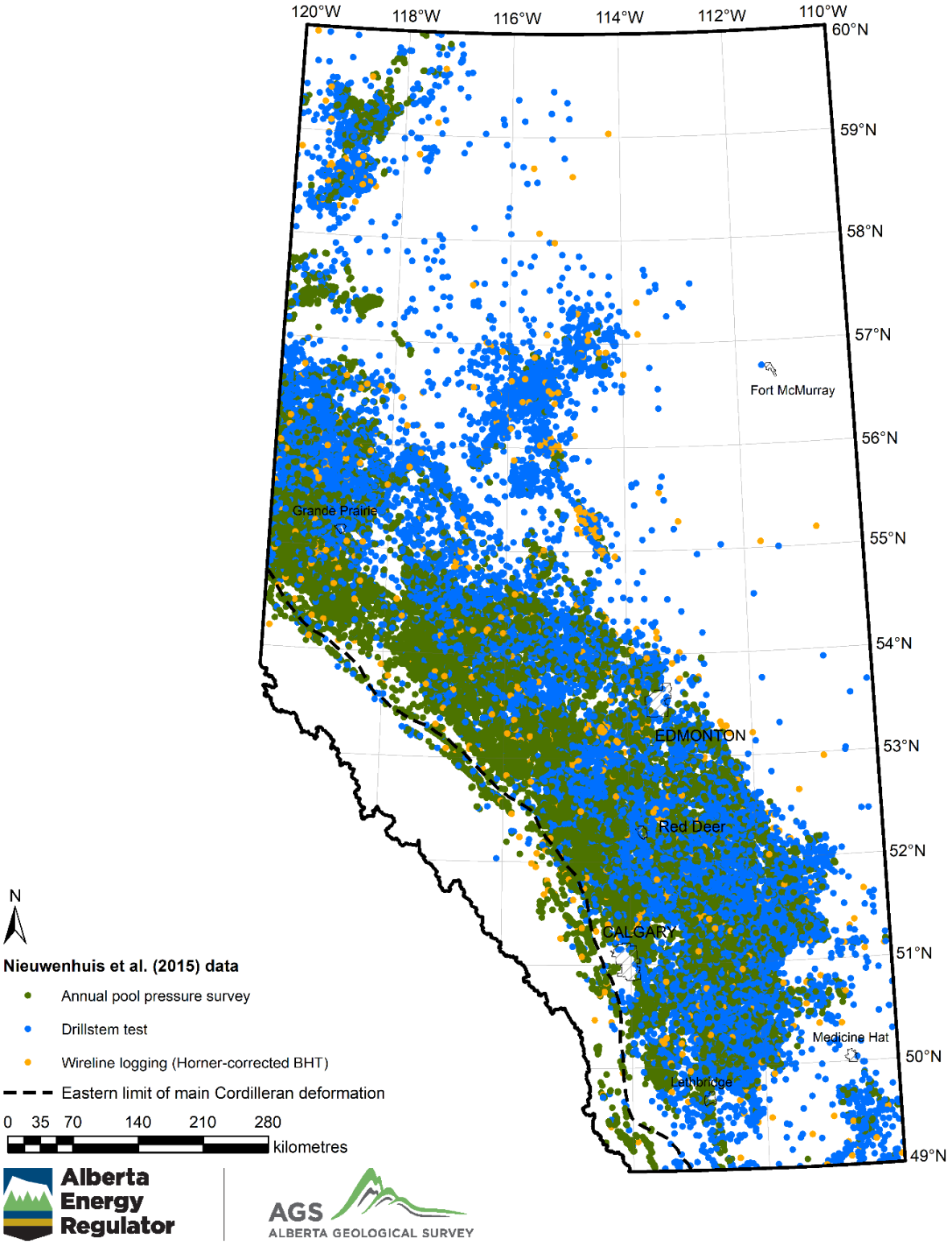

Figure 10. Locations of recorded temperatures, included in the Nieuwenhuis et al. (2015) dataset. This dataset was combined with the Alberta-calibrated Harrison-corrected bottomhole temperature (BHT) dataset (Figure 11) and used to create an updated temperature model.

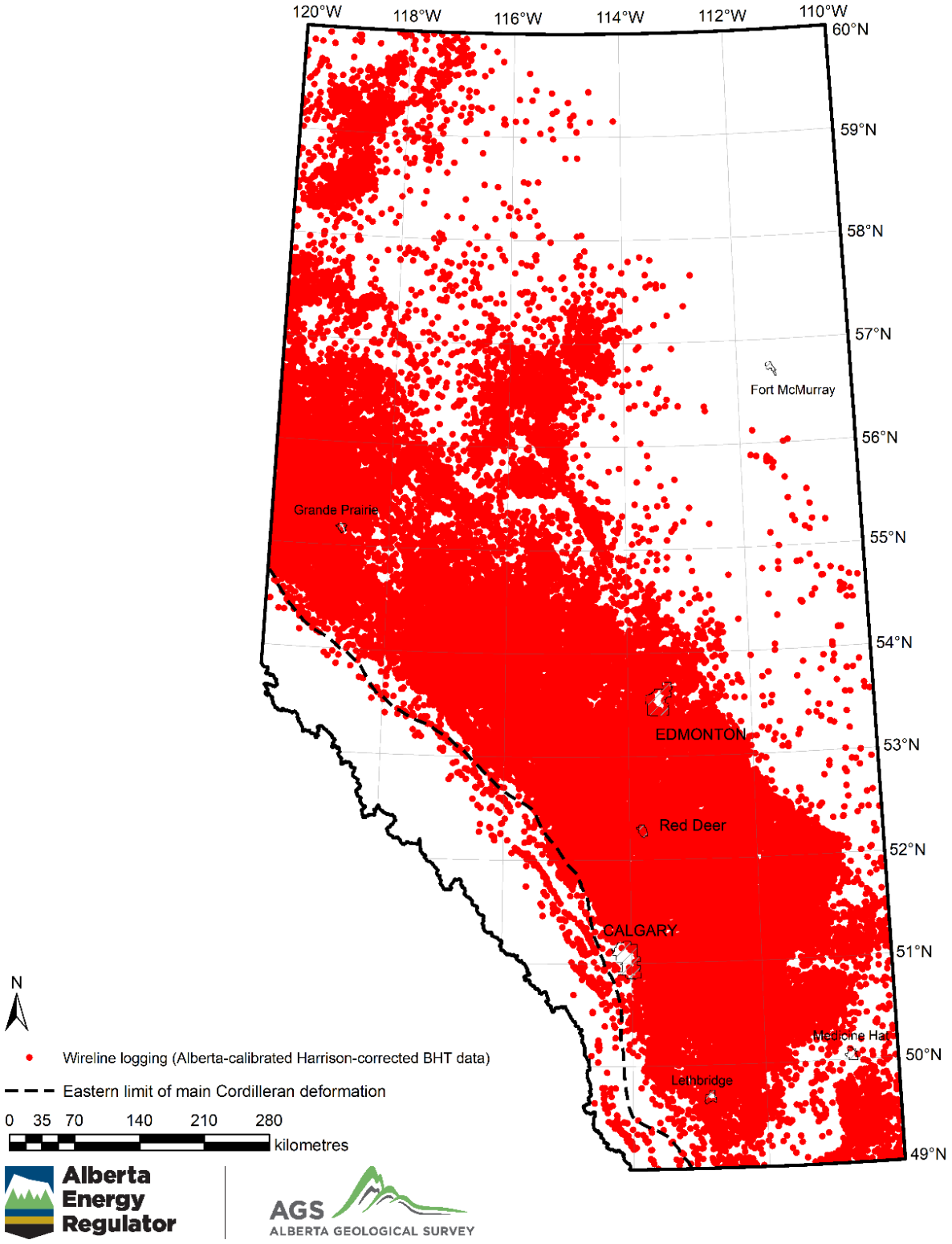

Figure 11. Locations of recorded temperatures, included in the Alberta-calibrated Harrison-corrected bottomhole temperature (BHT) dataset. This dataset was added to the Nieuwenhuis et al. (2015) dataset (Figure 10) and used to create an updated temperature model.

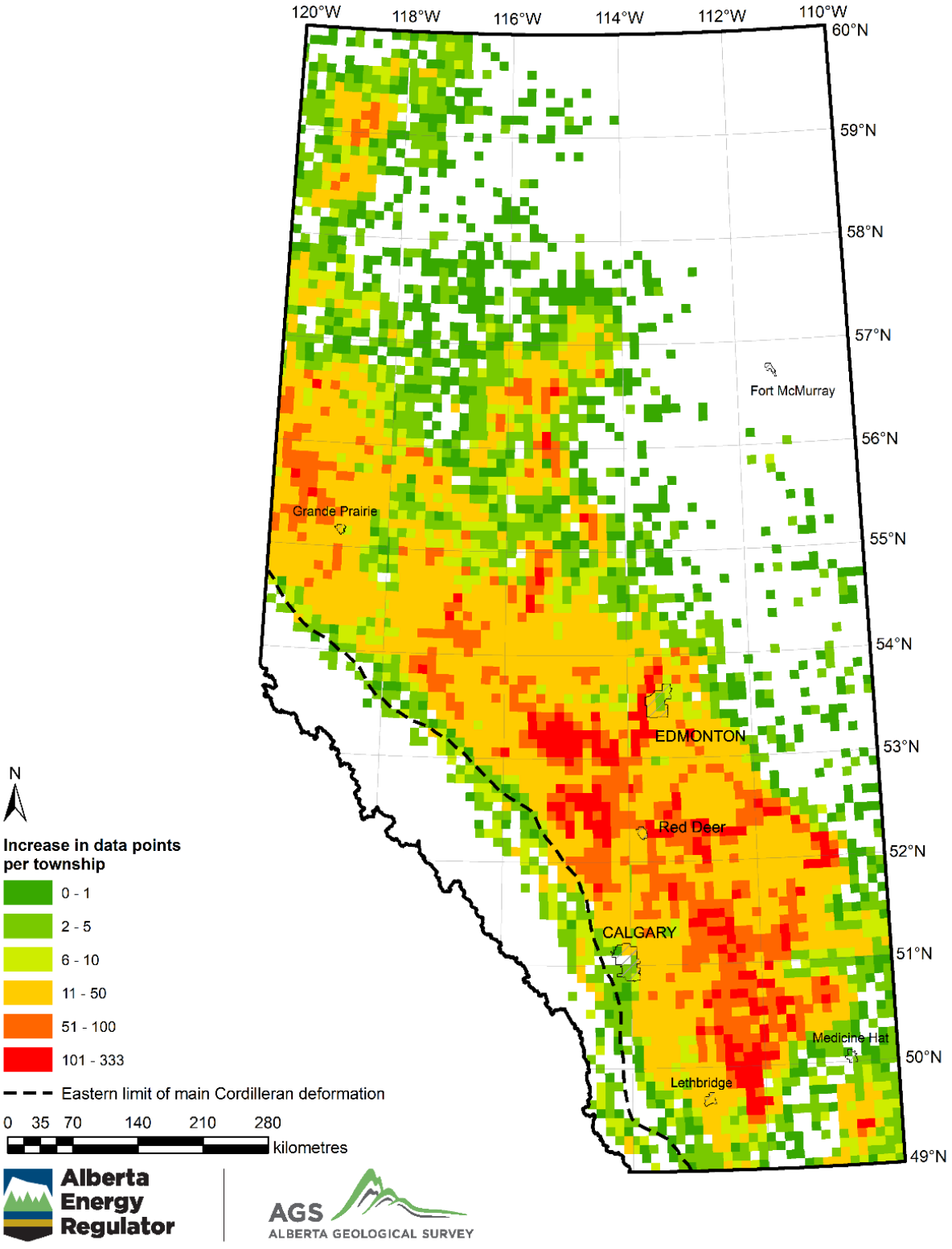

Figure 12. Increase in data points per township resulting from the addition of the bottomhole temperature dataset to the Nieuwenhuis et al. (2015) dataset. Both datasets were used to create an updated temperature model.

Table 3. Temperature distribution summary for formation/group-scale maps created from the updated temperature model. Each section of a township equals 2.59 km^2.

Geological Unit	Maximum Depth (m)	Total No. of Sections at >1000 m Depth	<40°C (no. of sections)	40–70°C (no. of sections)	70–100°C (no. of sections)	100–150°C (no. of sections)	>150°C (no. of sections)
Base of Wabamun Group	5578	112 000	20 353	45 941	28 523	16 903	280
Base of Winterburn Group	5848	109 225	15 718	47 519	28 697	16 769	522
Base of Leduc Formation	6050	52 408	1 396	32 461	10 916	7 142	493
Base of contiguous Swan Hills and Slave Point formations	6223	146 231	13 959	71 463	37 770	21 650	1 389
Base of Watt Mountain Formation	6707	142 697	13 305	70 316	36 702	21 473	901
Base of Sulphur Point Formation	2814	14 269	0	6 483	6 861	925	0
Base of Keg River Formation	3712	93 383	13 626	57 886	17 713	4 158	0
Top of Precambrian basement	6723	193 184	14 493	87 715	52 801	35 828	2 347

6 Summary

Results of this project include a new Alberta-calibrated Harrison equation, which can be used to correct bottomhole temperatures to the in situ formation temperature. This correction equation was applied to previously unused bottomhole temperature data, which were then merged with a pre-existing temperature dataset to create an updated database of subsurface temperatures in Alberta. This new equation could also be applied to temperatures recorded at depths greater than 1000 m in new wells drilled with mud circulating fluids in the province of Alberta.

Temperature maps for select Devonian units were produced (Wabamun and Winterburn groups, and Leduc, Swan Hills / Slave Point, Watt Mountain, Keg River, and Sulphur Point formations) as well as for the base of the sedimentary succession (top of the Precambrian). An updated thermal gradient map provides an estimate of the average temperature increase with depth to the top of the Precambrian basement. Although this gradient map assumes a linear geothermal gradient from the surface to the basement, point cloud data from the three-dimensional model can be sampled every 4000 m in the x,y direction and every 125 m in the z direction providing more detailed temperature predictions. Grid products exported from this model were expanded to include five formations and one group spanning from the uppermost Devonian to the Jurassic.

7 References

Alberta Energy Regulator (2021): Directive 040: Pressure and Deliverability Testing Oil and Gas Wells; URL <https://static.aer.ca/prd/documents/directives/Directive040.pdf> [February 2022].

Alberta Energy Regulator (2022): Products and Services Catalogue - Well Logs; URL <https://www1.aer.ca/productcatalogue/230.html> [February 2022].

Alberta Geological Survey (2021): Geological Framework of Alberta, version 3 (interactive app and map, methodology, model, dataset, story maps, web maps); Alberta Energy Regulator / Alberta Geological Survey, AER/AGS Interactive Application, URL <https://gfa-v3-ags-aer.hub.arcgis.com> [December 2021].

Brinsky, J., Singh, A., Hauck, T.E., Grobe, M. and Palombi, D. (2022a): Subsurface temperature model of Alberta: input data (tabular data, tab-delimited format); Alberta Energy Regulator / Alberta Geological Survey, AER/AGS Digital Data 2021-0029, URL <https://ags.aer.ca/publication/dig-2021-0029>.

Brinsky, J., Singh, A., Hauck, T.E., Grobe, M. and Palombi, D. (2022b): Subsurface temperature model of Alberta: point cloud data; Alberta Energy Regulator / Alberta Geological Survey; AER/AGS Digital Data 2021-0030, URL <https://ags.aer.ca/publication/dig-2021-0030>.

Brinsky, J., Singh, A., Hauck, T.E., Grobe, M. and Palombi, D. (2022c): Temperature mapping of select geological strata in Alberta (gridded data, ASCII format); Alberta Energy Regulator / Alberta Geological Survey, AER/AGS Digital Data 2021-0031, URL <https://ags.aer.ca/publication/dig-2021-0031>.

Bachu, S. and Burwash, R.A. (1994): Geothermal regime in the Western Canada Sedimentary Basin; *in* Geological atlas of the Western Canada Sedimentary Basin, G.D. Mossop and I. Shetsen (comp.), Canadian Society of Petroleum Geologists and Alberta Research Council, p. 447–453, URL <https://ags.aer.ca/atlas-the-western-canada-sedimentary-basin/chapter-30-geothermal-regime> [February 2022].

Banks, J. and Harris, N.B. (2018): Geothermal potential of foreland basins: a case study from the Western Canadian Sedimentary Basin; Geothermics, v. 76, p. 74–92.

DeFord, R.K. and Kehle, R.O. (1976): Geothermal gradient map of North America; American Association of Petroleum Geologists and U.S. Geological Survey, scale 1:5 000 000.

Gray, A., Majorowicz, J. and Unsworth, M. (2012): Investigation of the geothermal state of sedimentary basins using oil industry thermal data: case study from northern Alberta exhibiting the need to systematically remove biased data; Journal of Geophysics and Engineering, v. 9, p. 534–548, URL <https://academic.oup.com/jge/article/9/5/534/5128849> [December 2021].

Harrison, W.E., Luza, K.V., Prater, M.L. and Chueng, P.K. (1983): Geothermal resource assessment of Oklahoma; Oklahoma Geological Survey, Special Publication 83-1, 42 p.

Horner, D.R. (1951): Pressure build-up in wells; 3rd World Petroleum Congress, May 28–June 6, 1951, The Hague, The Netherlands.

Jones, F.W., Lam, H.-L. and Majorowicz, J.A. (1985): Temperature distributions at the Paleozoic and Precambrian surfaces and their implications for geothermal energy recovery in Alberta; Canadian Journal of Earth Sciences, v. 22, p. 1774–1780.

Kehle, R.O., Schoeppel, R.J. and Deford, R.K. (1970): The AAPG geothermal survey of North America; Geothermics, v. 2, pt. 1, p. 358–367, doi:10.1016/0375-6505(70)90034-9.

Kent, D.M. and Christopher, J.E. (1994): Geological history of the Willison Basin and Sweetgrass Arch; *in* Geological atlas of the Western Canada Sedimentary Basin, G.D. Mossop and I. Shetsen (comp.), Canadian Society of Petroleum Geologists and Alberta Research Council, p. 421–429, URL <https://ags.aer.ca/atlas-the-western-canada-sedimentary-basin/chapter-27-williston-basin-and-sweetgrass-arch> [December 2021].

Lam, H.-L. and Jones, F. (1985): Geothermal energy potential in the Hinton-Edson area of west-central Alberta; Canadian Journal of Earth Sciences, v. 22, p. 369–383, doi:10.1139/e85-036.

Lam, H.L. and Jones, F. (1986): An investigation of the potential for geothermal energy recovery in the Calgary area in southern Alberta, using petroleum exploration data; Geophysics, v. 51, p. 1661–1670.

Lengyel, T. (2013): Geothermics of the Phanerozoic strata of Saskatchewan; M.Sc. thesis, University of Alberta.

Majorowicz, J.A., Unsworth, M., Chacko, T., Gray, A., Heaman, L., Potter, D., Schmitt, D. and Babadagli, T. (2012): Geothermal energy as a source of heat for oil sands processing in northern Alberta, Canada; *in* Heavy-oil and oil sand petroleum systems in Alberta and beyond, F.J. Hein, D. Leckie, S. Larter and J. Suter (ed.), American Association of Petroleum Geologists, Studies in Geology, v. 64, p. 1–22.

Nieuwenhuis, G., Lengyel, T., Majorowicz, J.A., Grobe, M., Rostron, B., Unsworth, M.J. and Weides, S. (2015): Regional-scale geothermal exploration using heterogeneous industrial temperature data; a case study from the Western Canadian Sedimentary Basin; *in* Proceedings of the World Geothermal Congress, April 16–24, 2015, Melbourne, Australia, p. 19–25.

O'Connell, S.C. (1994): Geological history of the Peace River Arch; *in* Geological atlas of the Western Canada Sedimentary Basin, G. Mossop and I. Shetsen (comp.), Canadian Society of Petroleum Geologists and Alberta Research Council, p. 431–437, URL <https://ags.aer.ca/atlas-the-western-canada-sedimentary-basin/chapter-28-geological-history-the-peace-river-arch> [February 2022].

U.S. Geological Survey (2014): Shuttle radar topography mission digital elevation model data (1-arc second resolution); Earth Resources Observation and Science Center, URL <http://earthexplorer.usgs.gov> [January 2015].

Weides, S. and Majorowicz, J.A. (2014): Implications of spatial variability in heat flow for geothermal resource evaluation in large foreland basins: the case of the Western Canada Sedimentary Basin; Energies, v. 7, p. 2573–2594, doi:10.3390/en7042573.

Weides, S., Moeck, I., Majorowicz, J.A., Palombi, D. and Grobe, M. (2013): Geothermal exploration of Paleozoic formations in central Alberta; Canadian Journal of Earth Sciences, v. 50, p. 519–534.

Weides, S., Moeck, I., Majorowicz, J.A. and Grobe, M. (2014): The Cambrian Basal Sandstone Unit in central Alberta—an investigation of temperature distribution, petrography and hydraulic and geomechanical properties of a deep saline aquifer; Canadian Journal of Earth Sciences, v. 51, p.783–796.

Wright, G.N., McMechan, M.E. and Potter, D.E.G. (1994): Structure and architecture of the Western Canada Sedimentary Basin; *in* Geological atlas of the Western Canada Sedimentary Basin, G.D. Mossop and I. Shetsen (comp.), Canadian Society of Petroleum Geologists and Alberta Research Council, p. 25–40, URL <https://ags.aer.ca/atlas-the-western-canada-sedimentary-basin/chapter-3-structure-and-architecture> [February 2022].

Appendix 1 – Temperature Maps

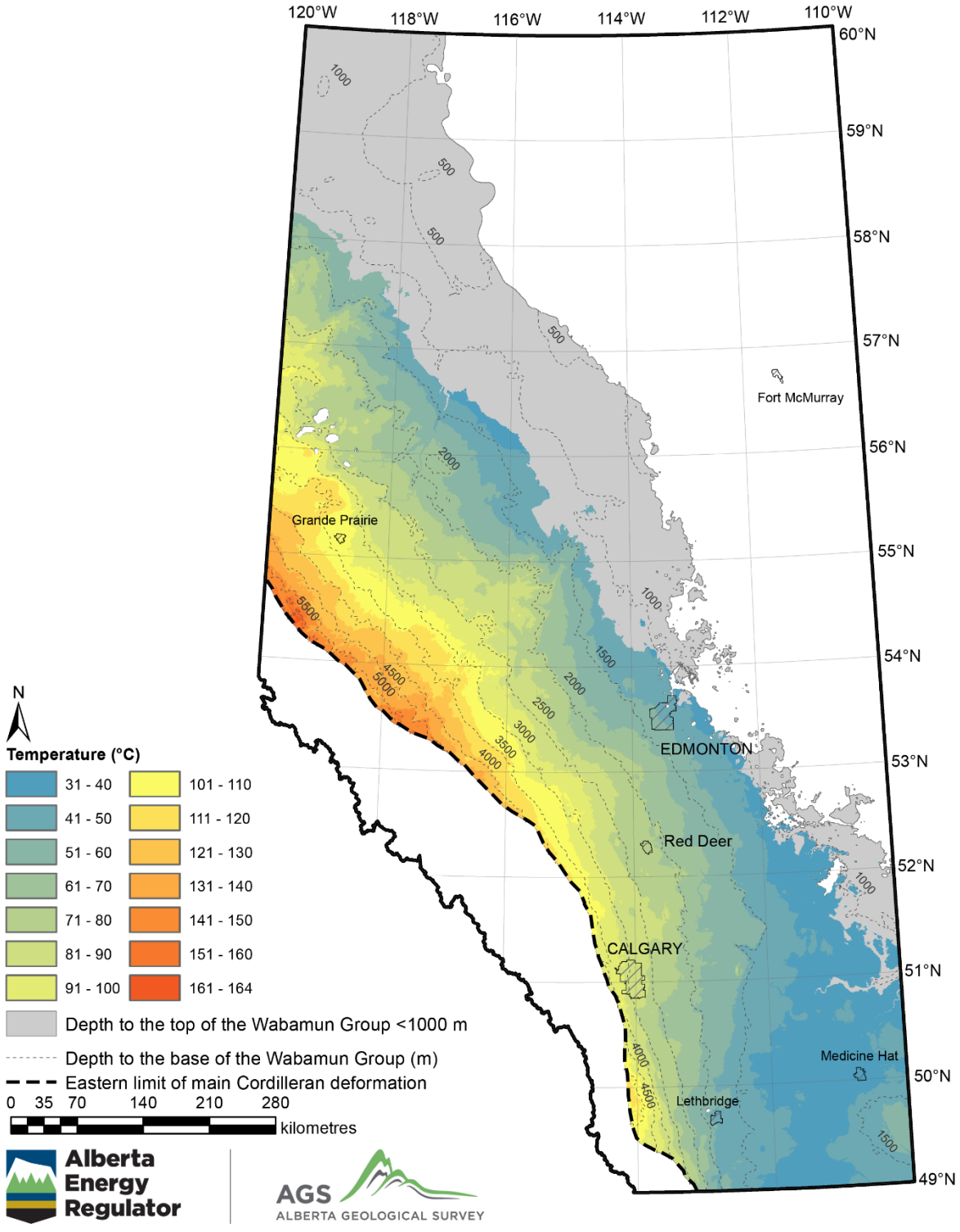

Figure 13. Temperature at the base of the Wabamun Group.

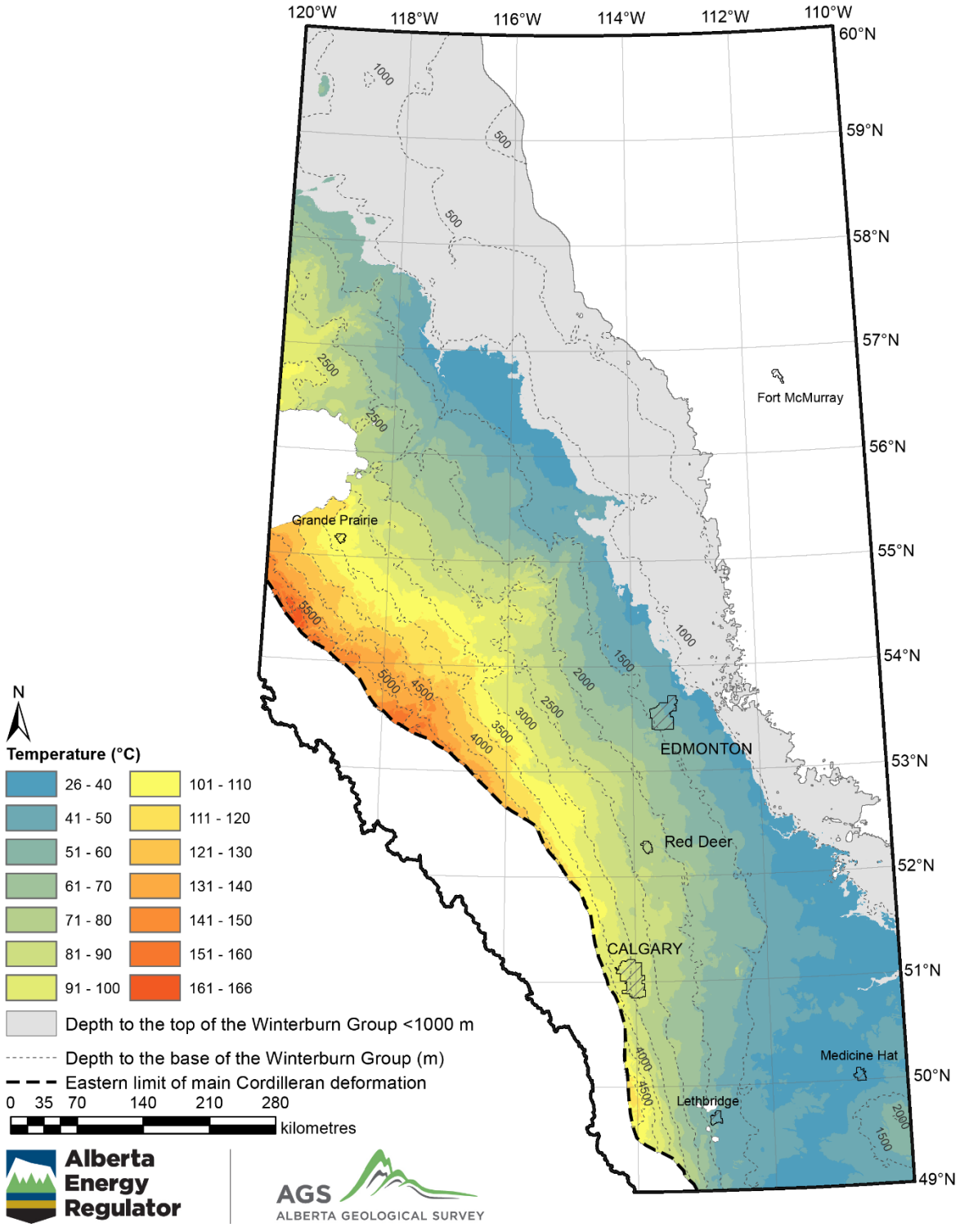

Figure 14. Temperature at the base of the Winterburn Group.

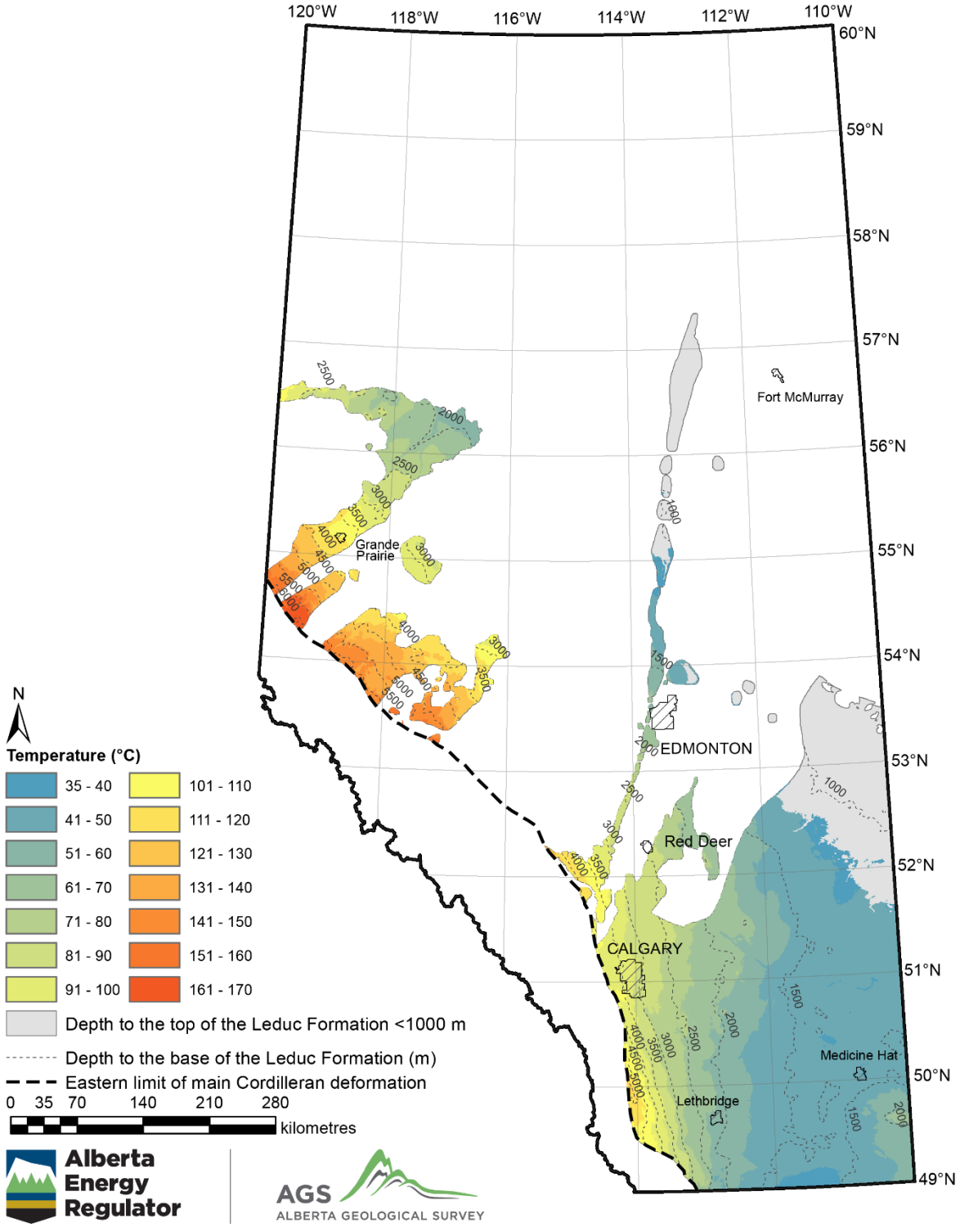

Figure 15. Temperature at the base of the Leduc Formation.

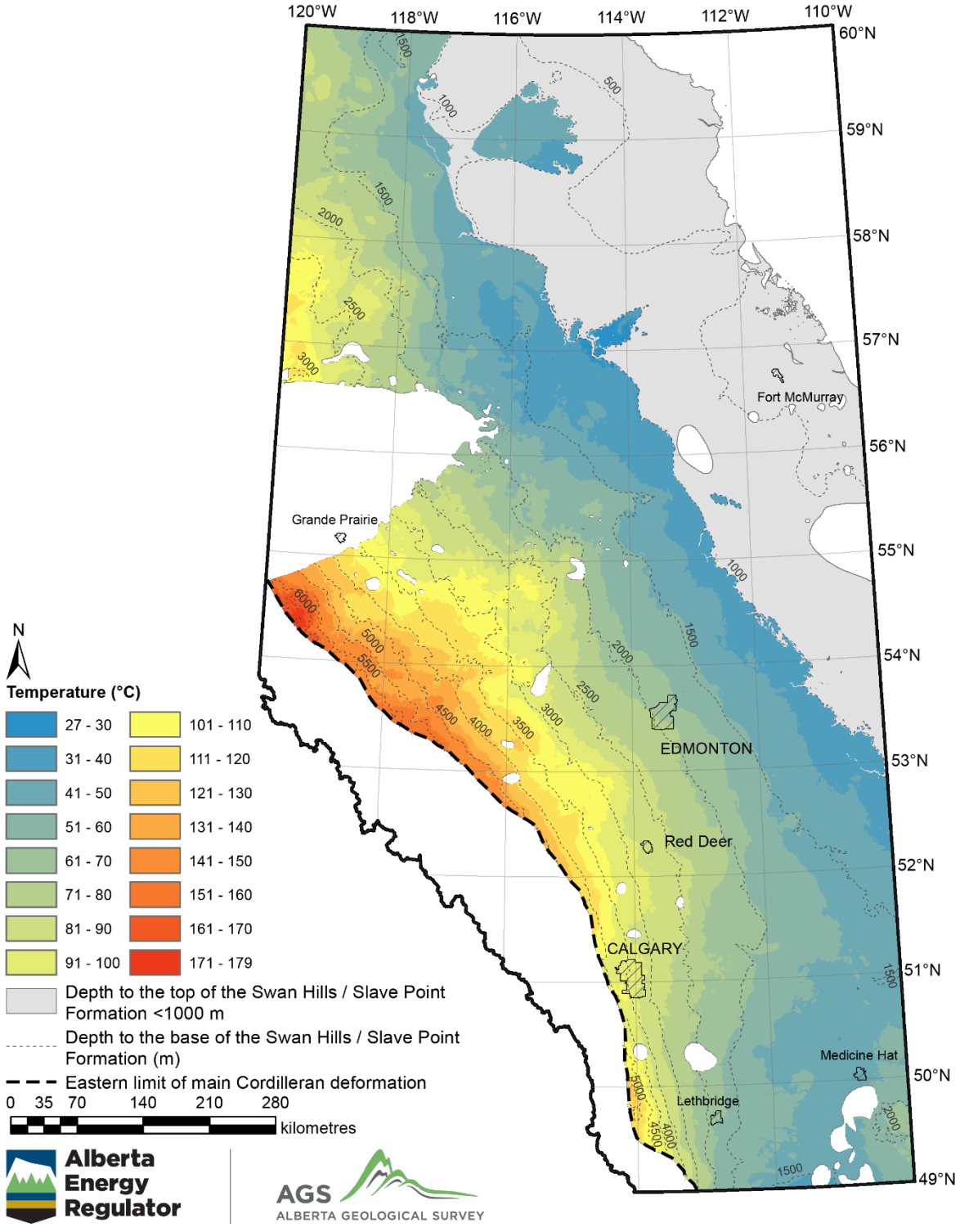

Figure 16. Temperature at the base of the contiguous Swan Hills and Slave Point formations.

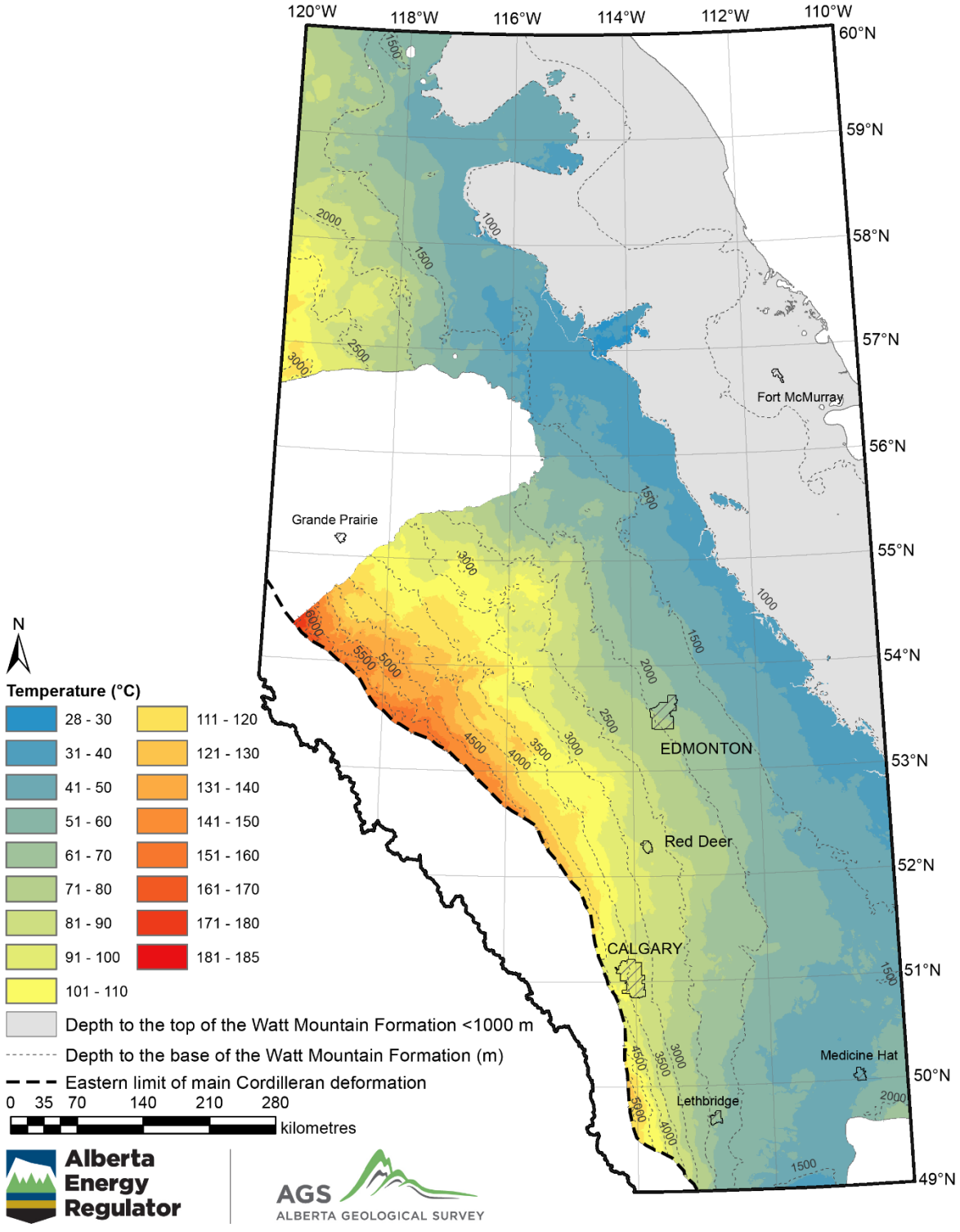

Figure 17. Temperature at the base of the Watt Mountain Formation.

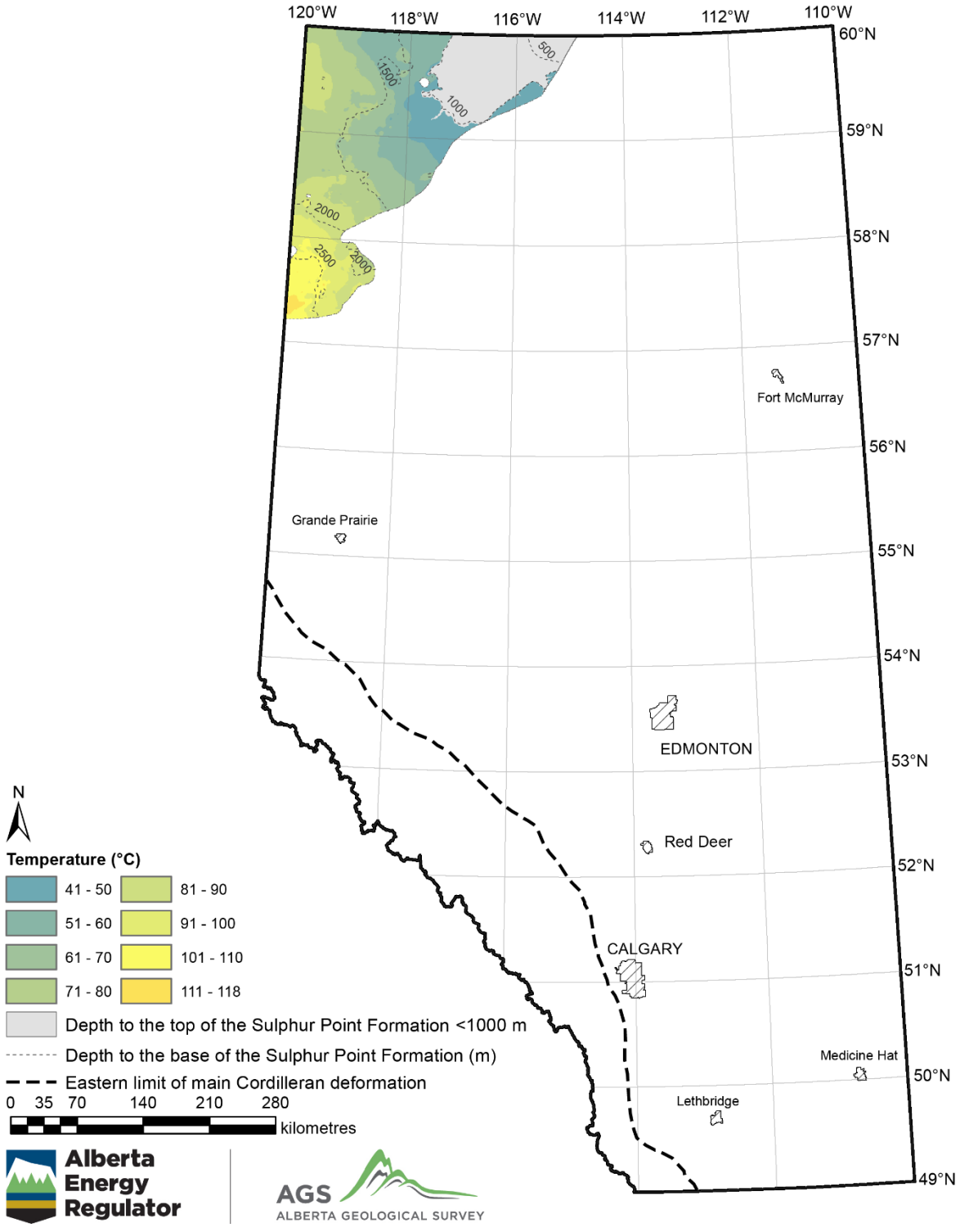

Figure 18. Temperature at the base of the Sulphur Point Formation.

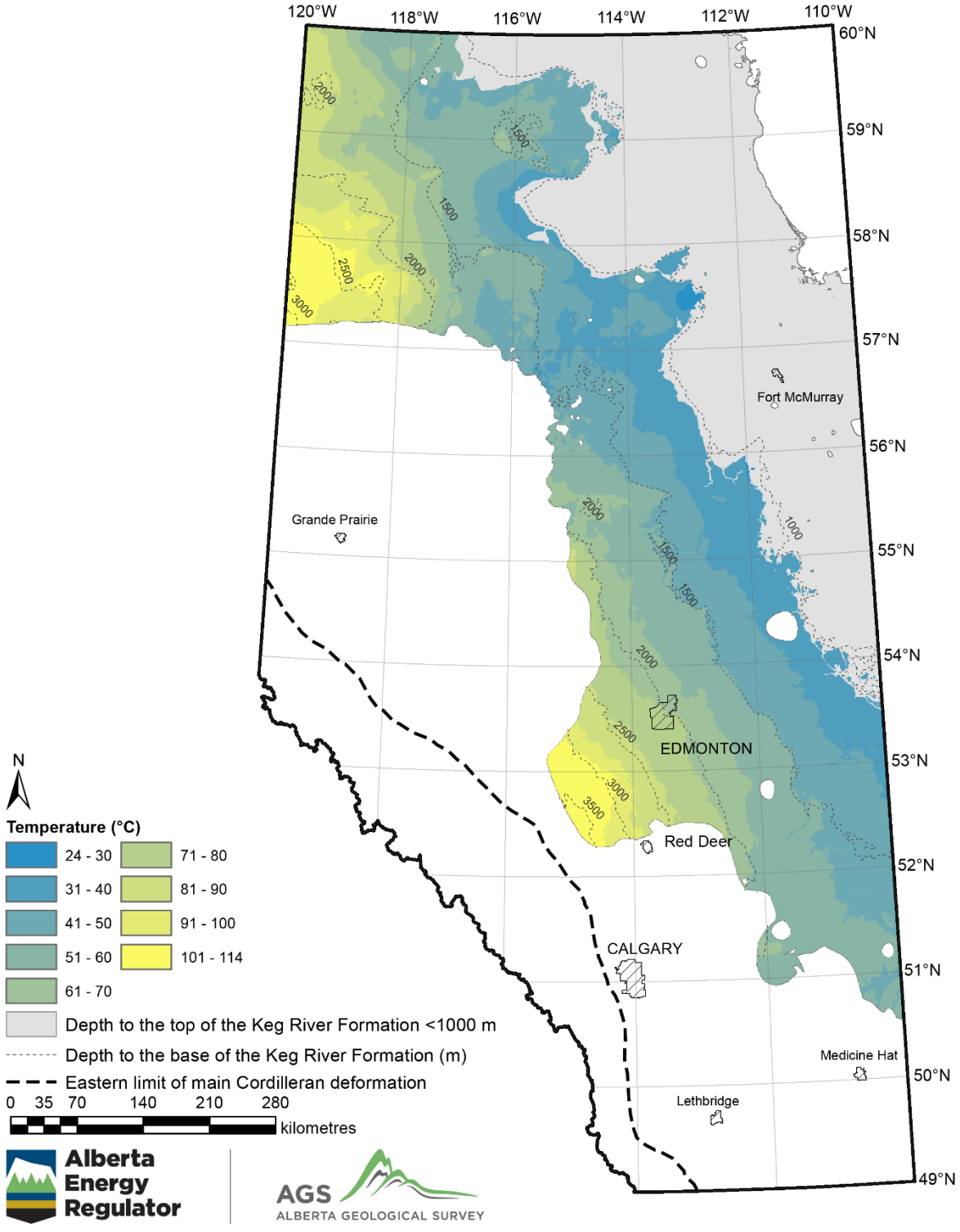

Figure 19. Temperature at the base of the Keg River Formation.

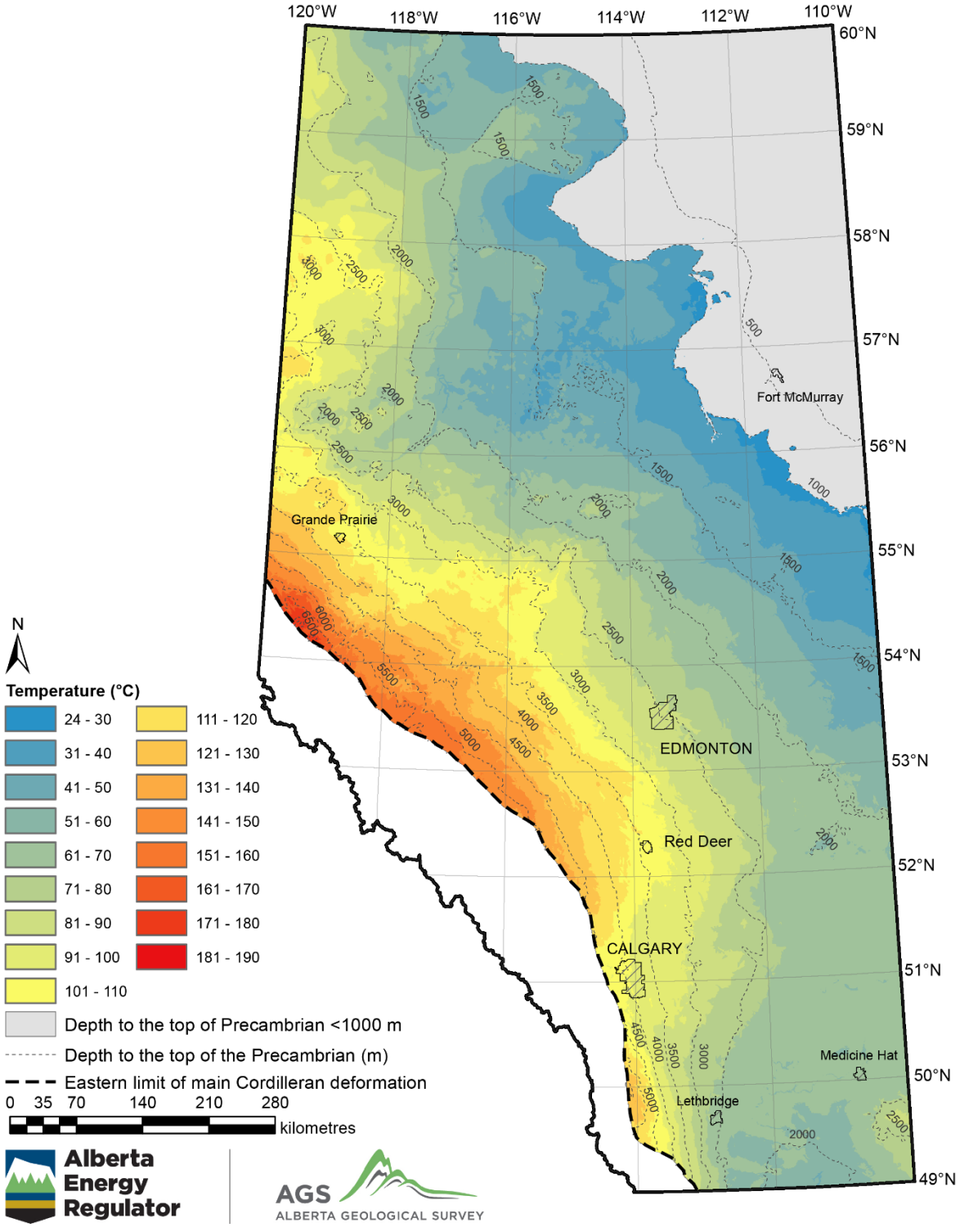

Figure 20. Temperature at the top of the Precambrian.

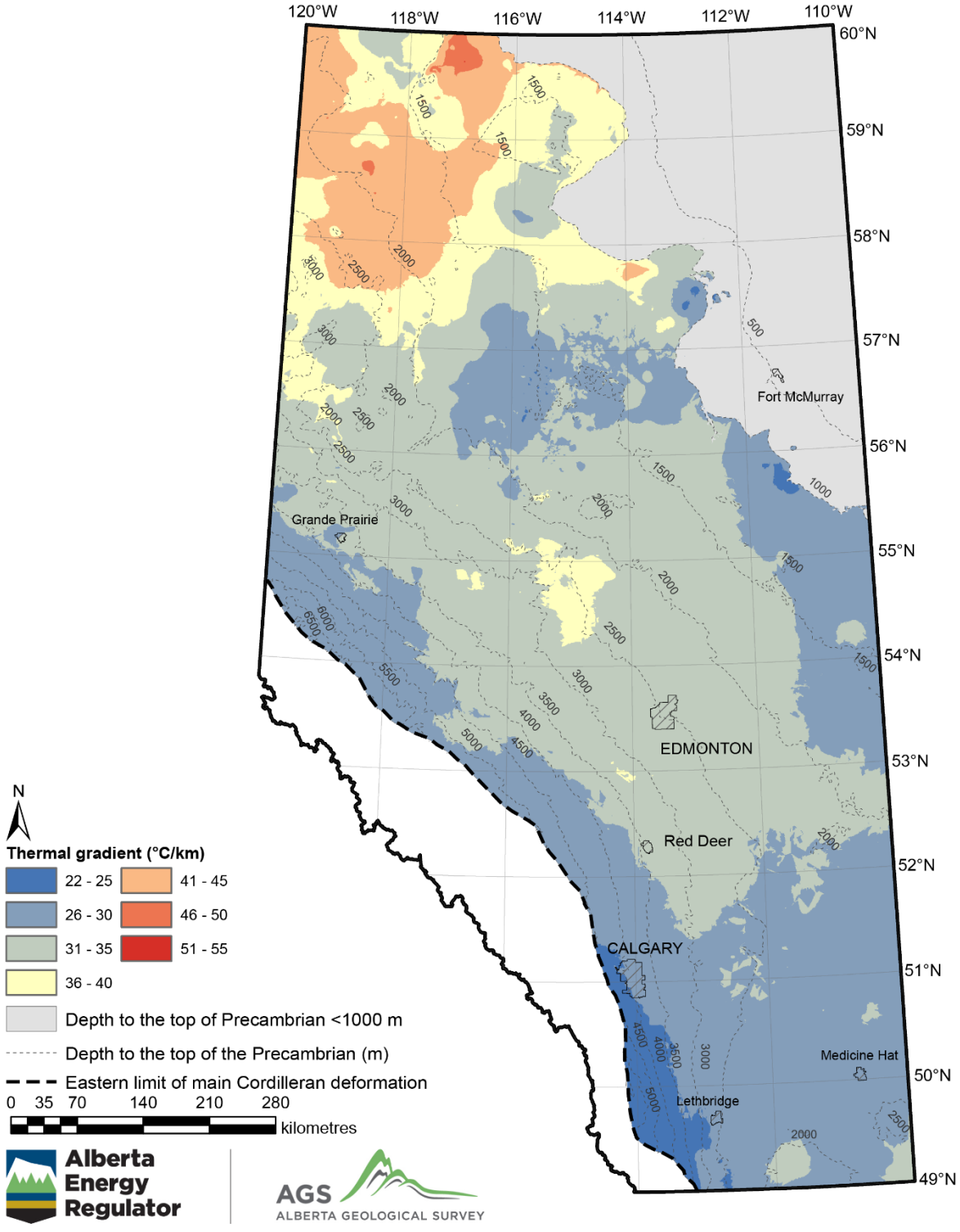

Figure 21. Thermal gradient calculated at the top of the Precambrian.